

Received: 2019.12.02
Accepted: 2020.01.13
Published: 2020.01.28

Downregulated miR-524-5p Participates in the Tumor Microenvironment of Ameloblastoma by Targeting the Interleukin-33 (IL-33)/Suppression of Tumorigenicity 2 (ST2) Axis

Authors' Contribution:
Study Design A
Data Collection B
Statistical Analysis C
Data Interpretation D
Manuscript Preparation E
Literature Search F
Funds Collection G

A 1 **Lijie Chen***
B 1 **Guannan Wang***
C 2 **Xue Qiao**
D 1 **Xiaobin Wang**
E 1 **Jinwen Liu**
F 1 **Xing Niu**
AG 1,3 **Ming Zhong**

1 Department of Oral Histopathology, School of Stomatology, China Medical University, Shenyang, Liaoning, P.R. China
2 Department of Central Laboratory, School of Stomatology, China Medical University, Shenyang, Liaoning, P.R. China
3 Department of Stomatology, Xiang'an Hospital of Xiamen University, Xiamen, Fujian, P.R. China

* Lijie Chen and Guannan Wang are equal contributors

Corresponding Author: Ming Zhong, e-mail: mzhong@cmu.edu.cn

Source of support: This work was funded by the National Natural Science Foundation of China (81072197 and 81470758)

Background: Ameloblastoma (AB) is a common odontogenic epithelial tumor, with locally invasive behavior and high recurrence. In this study, we hypothesized that miR-524-5p could be involved in the tumor microenvironment by targeting interleukin-33 (IL-33)/suppression of tumorigenicity 2 (ST2) in AB.

Material/Methods: The microRNA (miRNA) expression profile of AB tissues and normal oral mucosa tissues (NOM; 6 paired samples) was analyzed. The miRNAs with fold change ≥ 2 and $P < 0.05$ were considered to be differentially expressed. Among them, downregulated miR-524-5p was verified by real-time qPCR. Potential targets of miR-524-5p were predicted by bioinformatics analysis. The expression levels of target genes were detected using real-time qPCR and Western blot, respectively. Immunohistochemistry analysis of target genes was performed, and we also assessed the correlation between miR-524-5p and its target.

Results: Microarray analysis results first indicated miR-524-5p is a downregulated miRNA in AB tissues. Real-time qPCR results confirmed the expression pattern of miR-524-5p in AB tissues. Moreover, IL-33 and its receptor ST2 were significantly overexpressed. As shown in immunohistochemistry results, IL-33 was positively expressed in lymphocytes and plasma cells, suggesting that IL-33/ST2 participates in tumor immune responses in the tumor microenvironment. Correlation analysis suggested that miR-524-5p expression was negatively correlated with IL-33/ST2.

Conclusions: Our findings reveal that downregulated miR-524-5p can participate in the tumor microenvironment of AB by targeting the IL-33/ST2 axis.

MeSH Keywords: **Ameloblastoma • Interleukins • MicroRNAs • Tumor Microenvironment**

Abbreviations: **AB** – ameloblastoma; **microRNA** – miRNA; **IL-33** – interleukin-33; **ST2** – suppression of tumorigenicity 2; **miRNA** – microRNA; **mRNAs** – messenger RNAs; **NOM** – normal oral mucosa; **IL-8** – interleukin-8

Full-text PDF: <https://www.medscimonit.com/abstract/index/idArt/921863>

 2228

 4

 7

 45



Background

AB is a common odontogenic epithelial neoplasm, characterized by locally invasive behavior and high recurrence (90%) [1,2]. AB accounts for around 1% of oral tumors and 11–18% of odontogenic tumors [3]. In 2005, the WHO classified AB into 4 types: solid/multicystic AB, peripheral AB, desmoplastic AB, and unicystic AB [4]. At present, the classification has been revised to AB, unicystic, and extraosseous/peripheral types [5,6]. To date, most molecular studies on AB have focused on exploring markers and genetic variation, which help to ensure diagnosis and better predict their prognosis [7–9]. Increasing evidence demonstrates that abnormal expression of multiple genes contributes to the development and progression of AB [10–12]. For example, a recent study found that FOXP1/SOX10 can distinguish AB from basaloid salivary gland tumors [13]. Furthermore, research at the molecular level helps advance precision medicine for AB. One study reported the successful treatment of patients with metastatic AB carrying the BRAF V600E mutation through BRAF-targeted therapies [14]. Therefore, it is necessary to further explore the pathogenesis of AB at the molecular level.

miRNAs are small non-coding RNAs that are 19–24 nucleotides in length [15]. They can mediate gene expression by binding to the 3'-untranslated region of target messenger RNAs (mRNAs), leading to translational repression or degradation of the target mRNAs [16,17]. It has been reported that miRNAs participate in biological processes, and their abnormal expression plays an important role in the development of cancers as oncogenes and suppressors [18]. Abnormally expressed miRNAs in cancer tissues compared with healthy tissues have been shown to be valuable biomarkers for the diagnosis and prognosis of cancers [19]. However, there is a lack of research analyzing the functions of altered miRNAs in AB tissues. Only 1 study analyzed miRNA expression profiles in solid and unicystic AB [20].

It has been confirmed that inflammation contributes to tumorigenesis [21]. The tumor microenvironment consists of immune cells, endothelial cells, pericytes, fibroblasts, and smooth muscle cells [22,23]. In the tumor microenvironment, inflammatory mediators are involved in promoting or inhibiting tumor immune responses. IL-33, a member of the IL-1 family, is secreted by necrotic epithelial cells and affects innate and adaptive immunity [24]. IL-33 mainly participates in the induction of type 2 immune responses through its receptor, ST2 [25]. IL-33/ST2 contributes to breast cancer [26], colorectal cancer [27], and gastric cancer [28]. However, the role of IL-33/ST2 has been not reported in AB and its underlying mechanism remains unclear.

Here, we analyzed miRNA profiles between AB and NOM tissues and identified underexpressed miR-524-5p in AB. We hypothesized that miR-524-5p is involved in the tumor microenvironment of AB by targeting IL-33/ST2 in AB.

Table 1. Patient demographics and clinical characteristics.

Clinicopathological characteristics	Number of case (n=90)
Age (years)	
<50	0
≥50	26
Gender	
Male	50
Female	40
Location	
Maxilla	8
Mandible	76
Pathological type	
Solid/multicystic	70
Peripheral	6
Desmoplastic	1
Unicystic	13
Recurrence	
Yes	9
No	81

Material and Methods

Tissue specimens

From 2014 to 2017, 29 cases of AB and 21 cases of NOM fresh tissues were randomly harvested from the oral and maxillofacial surgery of School of Stomatology, China Medical University. From 2015 to 2016, a total of 90 cases of formalin-fixed, paraffin-embedded (FFPE) AB tissues were randomly retrieved from the Department of Oral Histopathology, School of Stomatology, China Medical University (Table 1). Furthermore, 20 cases of NOM were obtained from the oral and maxillofacial surgery. The study was approved by the Ethics Committee of the School of Stomatology, China Medical University (2016-12). All patients signed informed consent.

Microarray analysis

Six cases of AB tissues and the corresponding NOM tissues were used for miRNA microarray analysis. The clinical information of the 6 patients with AB is shown in Table 2. Total RNA was extracted from tissues using TRIzol reagent (Invitrogen). RNA concentration and integrity were detected using a NanoDrop 1000 spectrophotometer.

Table 2. The clinical information of six patients with AB for microarray analysis.

Number	Age	Sex	Location	Pathological type	Recurrence or not
1	57	Male	Mandible	Solid/multicystic	Yes
2	47	Male	Mandible	Solid/multicystic	Yes
3	49	Female	Mandible	Solid/multicystic	No
4	45	Male	Mandible	Solid/multicystic	Yes
5	63	Female	Maxilla	Solid/multicystic	No
6	82	Male	Lip	Peripheral	No

Table 3. The primer sequences for Real-time qPCR.

Target	Primer sequences
miR-524-5p	5'-GTGCTCACTCCAGAGGGATG-3' (forward) 5'-TATGGTTGTTCCAGACTCCTTAC-3' (reverse)
U6	5'-ATTGGAACGATACAGAGAAGATT-3' (forward) 5'-GGAACGCTTCACGAATTTG-3' (reverse)
IL-33	5'-GTTGCATGCCAACACAAGGA-3' (forward) 5'-GCATTCAAATGAAACACAGTTGGAG-3' (reverse)
ST2	5'-GAGTTGTGAAACTGTGGGCAGAA-3' (forward) 5'-CACACATGAGGCAGTTGGTGATA-3' (reverse)
β-actin	5'-TGGCACCCAGCACAATGAA-3' (forward) 5'-CTAAGTCATAGCCGCTAGAAGCA-3' (reverse)

Real-time qPCR

Total RNA was extracted from tissues using TRIzol reagent. Then, all RNA was reverse-transcribed into cDNA using TaqMan real-time. For miR-524-5p detection, we used a stem-loop primer binding to the 3' portion of miR-524-5p. For mRNA detection, first-strand cDNA was synthesized by M-MLV reverse transcriptase using random primers. Then, the cDNA was mixed with primers for the real-time qPCR. The primer sequences of miR-524-5p, U6, IL-33, ST2, and β-actin are listed in Table 3. The relative expression level was calculated using $2^{-\Delta\Delta CT}$ method. U6 was used as an internal control for miR-524-5p, while β-actin was used as an internal control for IL-33 and ST2.

Bioinformatics prediction

The target gene of miR-524-5p was predicted using the TargetScanHuman 7.1 database.

Western blot analysis

We lysed 0.1 g tissues using 300 μl RIPA buffer supplemented with 3 μl 1% PMSF, and then centrifuged (12 000×g) samples for 5 min at 4°C. The protein in the supernatant was used for Western blot analysis. After separating SDS-PAGE by electrophoresis, the protein samples were transferred onto membranes.

Then, the membrane was blocked using 5% skimmed milk for 1 h. After incubation with primary antibodies at 4°C overnight, the membrane was incubated with secondary antibodies (1: 5000) for 50 min. The primary antibodies were rabbit anti-human IL-33 polyclonal antibody (Abcam, UK), and rabbit anti-human ST2 polyclonal antibody (Proteintech, USA). Finally, the protein was visualized using an infrared fluorescence scanning imaging system.

Immunohistochemistry

Paraffin-embedded tissue sections (thickness, 5 μm) were cut, dried, deparaffinized, and rehydrated following standard protocols [8]. Endogenous peroxidase was blocked with hydrogen peroxide (0.5% in methanol) for 15 min. Sections were incubated overnight with the primary antibodies goat anti-human IL-33 antibody (1: 100) and goat anti-human ST2 antibody (1: 100) at 4°C. Sections were incubated with the biotinylated secondary antibody for 10 min at 37°C. Then, sections were washed 3 times with PBS between each step, and DAB (Diarninobenzidin) substrate was used for visualization of immunoreactivity. Hematoxylin staining was then performed. For negative control, sections were treated as above but without the primary antibody. Isotype-matched mouse monoclonal IgG (Abcam) at appropriate concentrations (1: 1000 and 1: 50) was used in isotype controls. All control sections were negative.

Immunohistochemical assessment

The semiquantitative score standard of IL-33/ST2 expression was based on staining intensity and the percentage of positive cells. In a 200× field of view, each slice was randomly taken from 3 fields of view, and the staining intensity score and the percentage of positive tumor cells were scored: 0 was negative (–), and 1–4 was divided into weak positive (+), 5–8 is moderately positive (++) , and 9–12 is strongly positive (+++). The indicators that judge positive were jointly judged by 3 experts. Quantitative score standards were as follows: in the 200× field of view, each slice was randomly taken from 3 fields of view, with score 1=negative, score 2=low positive, score 3=positive, and score 4=high positive.

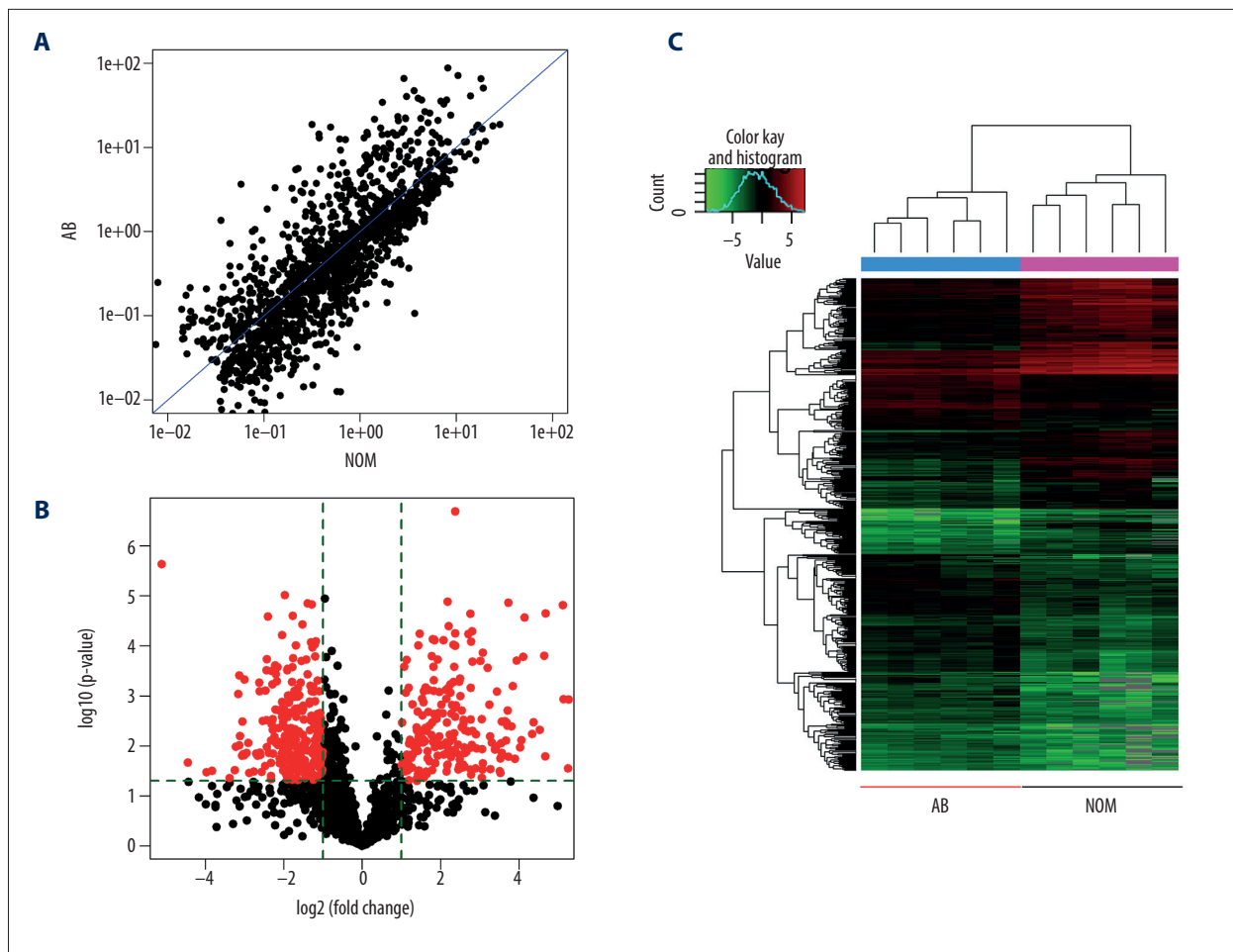


Figure 1. Differentially expressed miRNAs between AB and NOM tissues by microarray analysis. **(A)** The scatter plot shows the changes in the miRNA expression between the 2 groups. **(B)** The miRNA expression profile between the 2 groups is shown in the volcano plot. The vertical green lines suggest a 2-fold change in upregulated and downregulated miRNAs, respectively. The red points stand for differentially expressed miRNAs with fold change ≥ 2 and $P < 0.05$. **(C)** Hierarchical clustering demonstrates the differences in miRNA expression profiling between the 2 groups.

Statistical analysis

All statistical analyses were performed using GraphPad prism 7.0. Each experiment was independently repeated at least 3 times. The data are expressed as mean \pm standard deviation (SD). Two-group comparisons were determined using the *t* test, while multiple-group comparisons were performed using one-way ANOVA. P -value < 0.05 was considered statistically significant.

Results

miRNA expression profile in AB tissues

The miRNA expression profile in 6 pairs of AB tissues and NOM tissues was analyzed. The scatter plot shows the variation in miRNAs expression level between AB tissues and NOM

tissues (Figure 1A). Differentially expressed miRNAs were identified with the threshold of fold change ≥ 2 and $P < 0.05$. The volcano plot shows 2076 differentially expressed miRNAs between AB tissues and NOM tissues (Figure 1B). Hierarchical clustering demonstrates the differences of miRNA expression profiling between the 2 groups (Figure 1C). Among them, we found that downregulated miR-524-5p had the most significant difference between AB and NOM (fold change=0.11161652105589 and p -value=0.00091511012). Therefore, miR-524-5p was selected for further study.

miR-524-5p is downregulated in AB tissues

To validate the expression pattern of miR-524-5p, the cDNA of miR-524-5p in AB and NOM tissues was amplified by real-time qPCR (14 pairs). The results showed the expression of miR-524-5p in AB was significantly lower than that in NOM

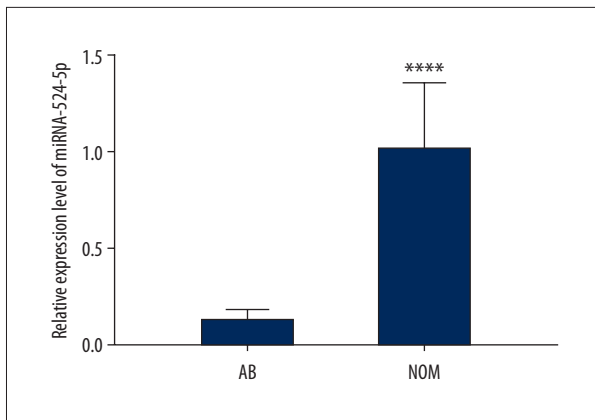


Figure 2. Real-time qPCR results show that miR-524-5p is downregulated in AB tissues compared to NOM tissues. **** $p < 0.0001$.

($P < 0.05$) (Figure 2). Therefore, miR-524-5p is downregulated in AB tissues compared with NOM tissues.

The high expression of IL-33 and its receptor ST2 in AB tissues

Bioinformatics predicted that IL-33 might become a target of miR-524-5p. The real-time qPCR was performed based on 15 AB specimens and 7 NOM specimens. The results showed that the expression of IL-33 in AB was 1.39 times higher than that in NOM ($P < 0.05$; Figure 3A), while the expression of ST2 in AB was 2.76 times higher than that in NOM ($P < 0.05$; Figure 3B). Western blot results showed that the expression of IL-33 in AB was 2.75 times higher than that in NOM ($P < 0.0001$; Figure 4A), while the expression of ST2 in AB was 2.16 times higher than that in NOM ($P < 0.0001$; Figure 4B).

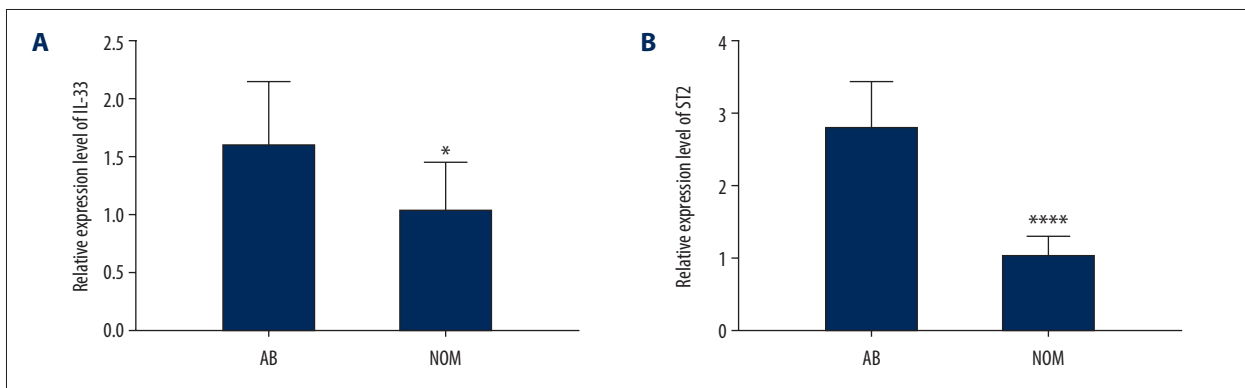


Figure 3. The real-time qPCR results show that IL-33 and its receptor ST2 are highly expressed in AB tissues compared to NOM tissues at the mRNA level. (A) IL-33; (B) ST2. * $p < 0.05$; **** $p < 0.0001$.

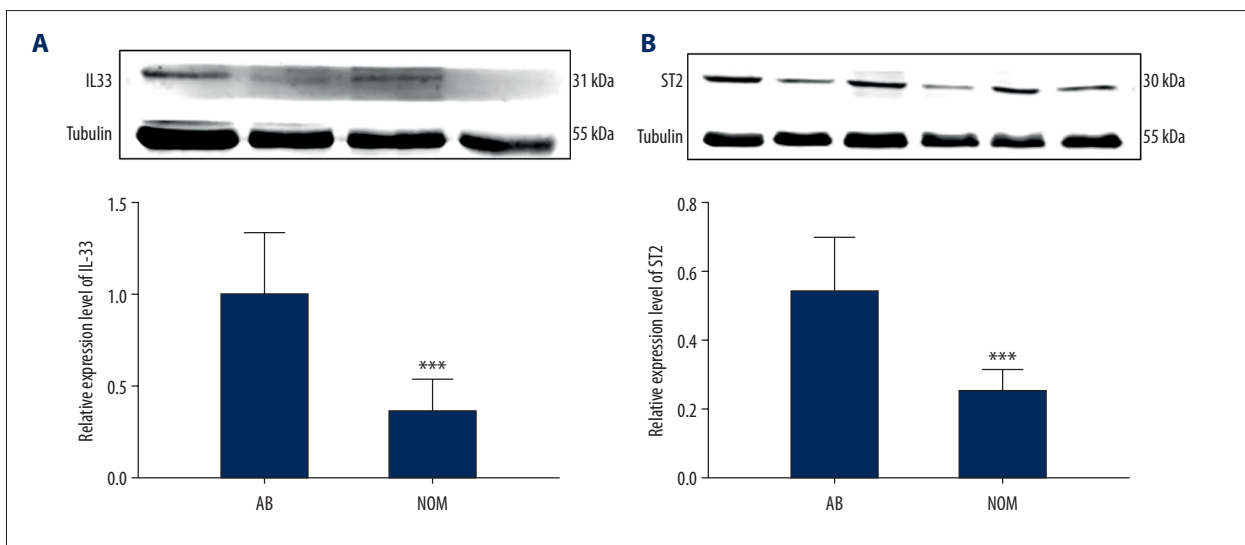


Figure 4. Western blot analysis results show that IL-33 and its receptor ST2 are highly expressed in AB tissues compared to NOM tissues at the protein level. (A) IL-33; (B) ST2. *** $p < 0.001$.

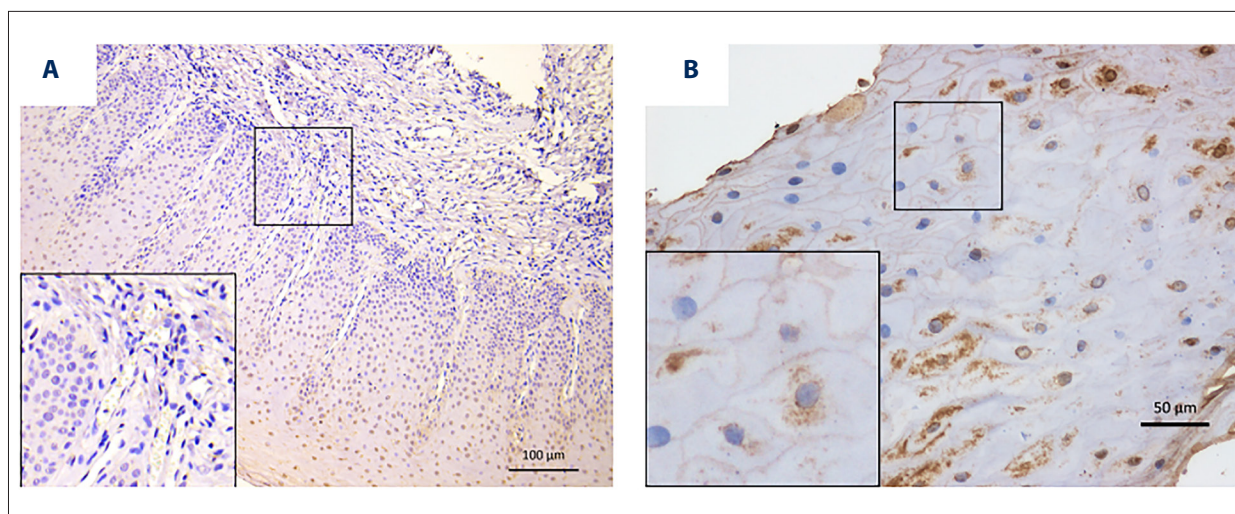


Figure 5. Immunohistochemistry results show the expression of (A) IL-33 and (B) ST2 in NOM.

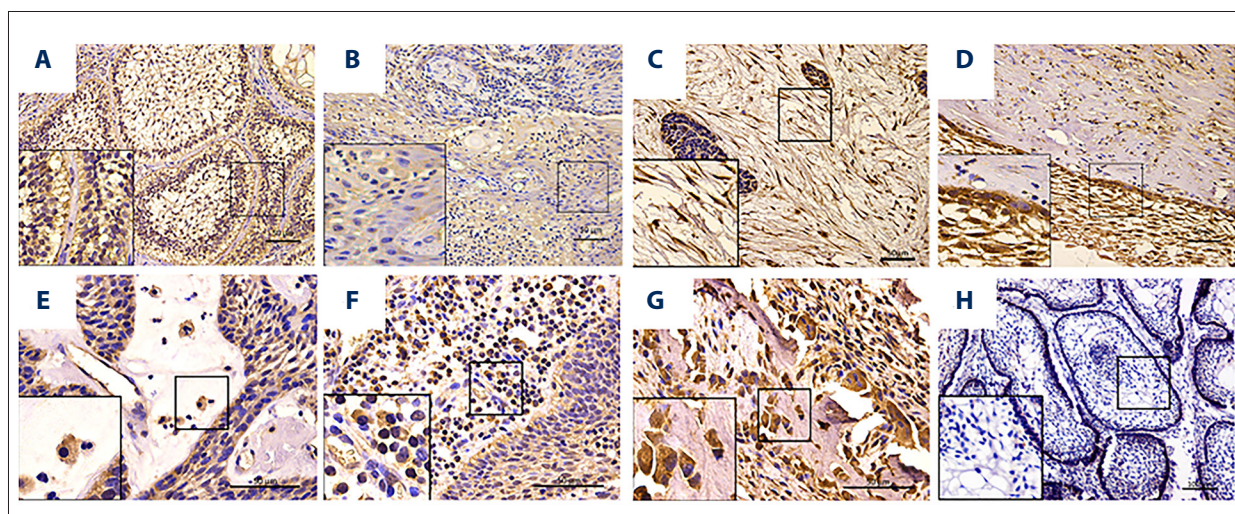


Figure 6. Immunohistochemistry results show the expression of IL-33 in AB. (A) Solid/multicystic AB (200×); (B) peripheral AB (200×); (C) desmoplastic AB (200×); (D) unicystic AB (200×); (E) monocyte (400×); (F) plasmacyte and lymphocyte (400×); (G) osteoclast (400×); (H) negative control (100×).

The correlation between miR-524-5p and IL-33/ST2

We found that expression of IL-33 was the opposite of the expression of miR-524-5p. Bioinformatics analysis showed that miR-524-5p has a binding site with IL-33. Therefore, Spearman correlation analysis was performed on the real-time qPCR results of 6 pairs of AB and NOM tissues. The results showed that there was a strong negative correlation between miR-524-5p and IL-33 expression in AB ($r=-0.886$, $P<0.05$).

The expression and distribution of IL-33/ST2 in AB tissues

Immunohistochemistry results showed that IL-33 and ST2 were negatively expressed in NOM (Figure 5A, 5B). IL-33 was mainly expressed in the nucleus of neoplastic epithelial cells. In

addition, IL-33 was positively expressed in inflammatory lymphocytes and plasma cells in the stroma. Occasionally, IL-33 was found in monocytes, endothelial cells, fibroblasts, and peripheral bones that are broken. In bone cells, IL-33 was positively expressed (Figure 6). ST2 was mainly distributed in the cytoplasm of neoplastic epithelial cells. Furthermore, ST2 was expressed in interstitial inflammatory lymphocytes and plasma cells. We also found that ST2 was present in monocytes, endothelial cells, fibroblasts, and pericardial osteoclasts (Figure 7). Combined with semiquantitative score, IL-33/ST2 were differentially expressed in AB and NOM ($P<0.05$). Moreover, IL-33/ST2 was significantly upregulated in AB (Table 4).

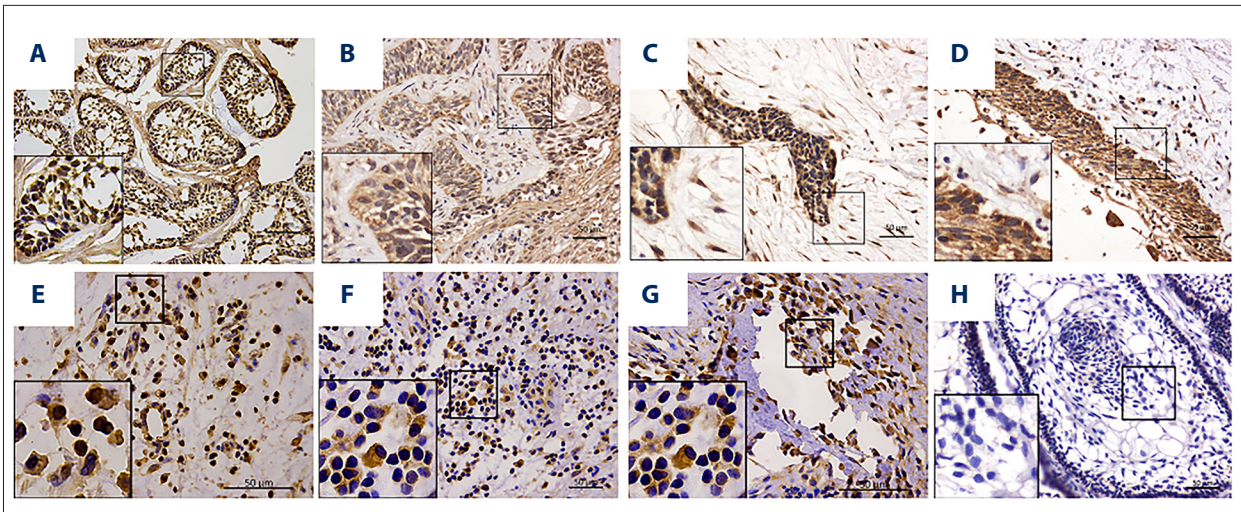


Figure 7. Immunohistochemistry results show the expression of ST2 in AB. (A) Solid/multicystic AB (200×); (B) peripheral AB (200×); (C) desmoplastic AB (200×); (D) unicystic AB (200×); (E) monocyte (400×); (F) plasmacyte and lymphocyte (400×); (G) osteoclast (400×); (H) negative control (200×).

Table 4. The difference of IL-33 and ST2 expression between AB and NOM tissues.

Group	IL-33 expression				P	ST2 expression				P
	+++	++	+	-		+++	++	+	-	
AB	12	41	34	3	<0.0001	11	28	47	4	<0.0001
NOM	0	2	12	6		1	3	11	5	

Discussion

In this study, we analyzed the miRNA expression profile of AB, and our findings revealed that miR-524-5p is involved in the tumor microenvironment of AB by the IL-33/ST2 axis, which provides a new insight into the mechanisms of AB.

We first analyzed the miRNA expression profile for AB tissues and NOM tissues. Among all differentially expressed miRNAs, we found the downregulated miR-524-5p in AB tissues. Consistent with microarray analysis results, real-time qPCR results confirmed that miR-524-5p was downregulated in AB tissues. Increasing evidence confirmed that miRNA-524 is involved in many human cancers. For example, Xu T et al. reported that miRNA-524 is downregulated in glioma and is associated with recurrence [29]. Furthermore, miRNA-524 can suppress the progression of glioma by directly targeting NCF2. Zhuang et al. found that miRNA-524 is upregulated in osteosarcoma, and its high expression promotes cell proliferation via inhibiting PTEN expression in osteosarcoma [30]. Downregulated miRNA-524 is identified in thyroid cancer, which can induce cell proliferation and suppresses cell apoptosis [31]. These studies suggest that the expression patterns of miRNA-524 are different in different cancers. In this study, our findings showed

that miR-524-5p was downregulated in AB tissues, indicating that low miR-524-5p expression might be involved in the development of AB.

As predicted by bioinformatics analysis, IL-33 could be considered as a potential target of miR-524-5p. Our real-time qPCR and Western blot analyses results showed that IL-33 and its receptor ST2 were upregulated in AB tissues, which is the opposite to miR-524-5p expression. These findings revealed that miR-524-5p is associated with the expression of IL-33 in AB tissues. It has been reported that high IL-33 expression is involved in the development of several cancers, such as pulmonary metastatic cancer and esophageal squamous cell carcinoma [32,33]. IL-33 is a major component in the tumor microenvironment. IL-33 can activate macrophages [34], dendritic cells [35], eosinophils [36], and neutrophils [36], all of which can enhance the tumor inflammatory microenvironment. Consistent with previous studies, our immunohistochemistry results showed that IL-33 was positively expressed in lymphocytes, plasma cells, monocytes, endothelial cells, and fibroblasts. These results indicate that IL-33 is involved in immune responses in the tumor microenvironment of AB. AB is triggered by mutations in key regulatory genes [37–39]. The tumor microenvironment, consisting of non-tumor cells and

molecules, also contributes to the progression of AB [40,41]. Studies have shown that when tissue damage, necrosis, or injury occur, IL-33 is rapidly released into the extracellular space and binds to ST2 on the target cell membrane, thereby activating T Helper 2 [42]. By recruiting immune cells, the IL-33/ST2 axis can reshape the tumor microenvironment to promote or resolve AB. Therefore, the IL-33/ST2 axis may be an effective regulator of the tumor microenvironment. In addition, IL-33 induces NF- κ B and MAPK activation by binding its receptor ST2 [25,43]. It has been found that NF- κ B and MAPK were abnormally expressed in AB [44,45], indicating that IL-33 can mediate the expression of NF- κ B and MAPK in AB. Our study indicated that downregulated miR-524-5p participates in the tumor microenvironment of AB by targeting the IL-33/ST2 axis.

References:

- Siar CH, Ng KH: Epithelial-to-mesenchymal transition in ameloblastoma: Focus on morphologically evident mesenchymal phenotypic transition. *Pathology*, 2019; 51: 494–501
- Nakano K, Takabatake K, Kawai H et al: Notch signaling affects oral neoplasm cell differentiation and acquisition of tumor-specific characteristics. *Int J Mol Sci*. 2019; 20: E1973
- Jhamb T, Kramer JM: Molecular concepts in the pathogenesis of ameloblastoma: Implications for therapeutics. *Exp Mol Pathol*, 2014; 97: 345–53
- Kim BK, Surti U, Pandya A et al: Clinicopathologic, immunophenotypic, and molecular cytogenetic fluorescence *in situ* hybridization analysis of primary and secondary cutaneous follicular lymphomas. *Am J Surg Pathol*, 2005; 29: 69–82
- El-Naggar AK, Chan JKC, Takata T et al: The fourth edition of the head and neck World Health Organization blue book: editors' perspectives. *Hum Pathol*, 2017; 66: 10–12
- Mascitti M, Togni L, Troiano G et al: Odontogenic tumours: A 25-year epidemiological study in the Marche region of Italy. *Eur Arch Otorhinolaryngol*, 2019 [Epub ahead of print]
- Wang GN, Zhong M, Chen Y et al: Expression of WNT1 in ameloblastoma and its significance. *Oncol Lett*, 2018; 16: 1507–12
- Gao X, Wang G, Zhang YK, Zhong M: Expression and mechanism of regulation of PP2A/Pr65 in ameloblastoma. *Surgeon*, 2014; 12: 129–33
- Zhong M, Wang J, Gong YB et al: [Expression of HOXC13 in ameloblastoma]. *Zhonghua Kou Qiang Yi Xue Za Zhi*, 2007; 42: 43–46 [in Chinese]
- Alsaegh MA, Altaie AM, Zhu S: p63 expression and its relation to epithelial cells proliferation in dentigerous cyst, odontogenic keratocyst, and ameloblastoma. *Pathol Oncol Res*, 2019 [Epub ahead of print]
- Liu X, Chen Z, Lan T et al: Upregulation of interleukin-8 and activin A induces osteoclastogenesis in ameloblastoma. *Int J Mol Med*, 2019; 43: 2329–40
- Zhang J, Wang Y, Fan C et al: Interleukin-8/beta-catenin mediates epithelial-mesenchymal transition in ameloblastoma. *Oral Dis*, 2019; 25(8): 1964–71
- Ko YCK, Varma S, Zhu CF et al: Gene expression profiling of head and neck tumors identifies FOXP1 and SOX10 expression as useful for distinguishing ameloblastoma from basaloid salivary gland tumors. *Am J Surg Pathol*, 2019 [Epub ahead of print]
- Brunet M, Khalifa E, Italiano A: Enabling precision medicine for rare head and neck tumors: The example of BRAF/MEK targeting in patients with metastatic ameloblastoma. *Front Oncol*, 2019; 9: 1204
- Rasnic R, Linial N, Linial M: Enhancing identification of cancer types via lowly-expressed microRNAs. *Nucleic Acids Res*, 2017; 45: 5048–60
- Bracken CP, Scott HS, Goodall GJ: A network-biology perspective of microRNA function and dysfunction in cancer. *Nat Rev Genet*, 2016; 17: 719–32
- Croce CM: Causes and consequences of microRNA dysregulation in cancer. *Nat Rev Genet*, 2009; 10: 704–14
- Slack FJ, Weidhaas JB: MicroRNA in cancer prognosis. *N Engl J Med*, 2008; 359: 2720–22
- Hayes J, Peruzzi PP, Lawler S: MicroRNAs in cancer: Biomarkers, functions and therapy. *Trends Mol Med*, 2014; 20: 460–69
- Setien-Olarrá A, Marichalar-Mendia X, Bediága NG et al: MicroRNAs expression profile in solid and unicystic ameloblastomas. *PLoS One*, 2017; 12: e0186841
- Wasmer MH, Krebs P: The role of IL-33-dependent inflammation in the tumor microenvironment. *Front Immunol*, 2016; 7: 682
- Grivennikov SI, Greten FR, Karin M: Immunity, inflammation, and cancer. *Cell*, 2010; 140: 883–99
- Koontongkaew S: The tumor microenvironment contribution to development, growth, invasion and metastasis of head and neck squamous cell carcinomas. *J Cancer*, 2013; 4: 66–83
- Liew FY, Girard JP, Turnquist HR: Interleukin-33 in health and disease. *Nat Rev Immunol*, 2016; 16: 676–89
- Schmitz J, Owyang A, Oldham E et al: IL-33, an interleukin-1-like cytokine that signals via the IL-1 receptor-related protein ST2 and induces T helper type 2-associated cytokines. *Immunity*, 2005; 23: 479–90
- Feng X, Liu H, Chu X et al: Recombinant virus-like particles presenting IL-33 successfully modify the tumor microenvironment and facilitate antitumor immunity in a model of breast cancer. *Acta Biomater*, 2019; 100: 316–25
- Landskron G, De la Fuente Lopez M, Dubois-Camacho K et al: Interleukin 33/ST2 axis components are associated to desmoplasia, a metastasis-related factor in colorectal cancer. *Front Immunol*, 2019; 10: 1394
- Eissmann MF, Dijkstra C, Jarnicki A et al: IL-33-mediated mast cell activation promotes gastric cancer through macrophage mobilization. *Nat Commun*, 2019; 10: 2735
- Xu T, Yu W, Li Q et al: MicroRNA-524 inhibits the progress of glioma via the direct targeting of NCF2. *Am J Transl Res*, 2019; 11: 1605–15
- Zhuang M, Qiu X, Cheng D et al: MicroRNA-524 promotes cell proliferation by down-regulating PTEN expression in osteosarcoma. *Cancer Cell Int*, 2018; 18: 114
- Nguyen PNN, Choo KB, Huang CJ et al: miR-524-5p of the primate-specific C19MC miRNA cluster targets TP53IP1- and EMT-associated genes to regulate cellular reprogramming. *Stem Cell Res Ther*, 2017; 8: 214
- Qi L, Zhang Q, Miao Y et al: Interleukin-33 activates and recruits natural killer cells to inhibit pulmonary metastatic cancer development. *Int J Cancer*, 2020; 146: 1421–34

Conclusions

Our study assessed the miRNA expression profiles of AB tissues. We found that miR-524-5p was downregulated in AB tissues compared to NOM tissues. Moreover, IL-33 and its receptor ST2 were highly expressed in AB tissues. According to immunohistochemistry results, IL-33/ST2 is involved in tumor immune responses in the tumor microenvironment. Further analysis of results showed that IL-33 was a potential target of miR-524-5p in AB. Therefore, our study reveals that downregulated miR-524-5p can participate in the tumor microenvironment of AB by targeting the IL-33/ST2 axis, which provides a novel insight into the mechanisms of AB.

Conflicts of interest

None.

33. Yue Y, Lian J, Wang T et al: IL-33-NF- κ B-CCL2 signaling pathway promotes the progression of esophageal squamous cell carcinoma by directing regulatory T cells. *Cancer Sci*, 2019 [Epub ahead of print]
34. Xu H, Sun L, He Y et al: Deficiency in IL-33/ST2 axis reshapes mitochondrial metabolism in lipopolysaccharide-stimulated macrophages. *Front Immunol*, 2019; 10: 127
35. Chen J, Zhao Y, Jiang Y et al: Interleukin-33 contributes to the induction of Th9 cells and antitumor efficacy by Dectin-1-activated dendritic cells. *Front Immunol*, 2018; 9: 1787
36. Lucarini V, Ziccheddu G, Macchia I et al: IL-33 restricts tumor growth and inhibits pulmonary metastasis in melanoma-bearing mice through eosinophils. *Oncoimmunology*, 2017; 6: e1317420
37. Brown NA, Rolland D, McHugh JB et al: Activating FGFR2-RAS-BRAF mutations in ameloblastoma. *Clin Cancer Res*, 2014; 20: 5517–26
38. Fregnani ER, Perez DE, Paes de Almeida O et al: BRAF-V600E expression correlates with ameloblastoma aggressiveness. *Histopathology*, 2017; 70: 473–84
39. Kurppa KJ, Caton J, Morgan PR et al: High frequency of BRAF V600E mutations in ameloblastoma. *J Pathol*, 2014; 232: 492–98
40. Fuchigami T, Kibe T, Koyama H et al: Regulation of IL-6 and IL-8 production by reciprocal cell-to-cell interactions between tumor cells and stromal fibroblasts through IL-1 α in ameloblastoma. *Biochem Biophys Res Commun*, 2014; 451: 491–96
41. Guzman-Medrano R, Arreola-Rosales RL, Shibayama M et al: Tumor-associated macrophages and angiogenesis: A statistical correlation that could reflect a critical relationship in ameloblastoma. *Pathol Res Pract*, 2012; 208: 672–76
42. Larsen KM, Minaya MK, Vaish V, Pena MMO: The role of IL-33/ST2 pathway in tumorigenesis. *Int J Mol Sci*, 2018; 19: E2676
43. Huang SJ, Yan JQ, Luo H et al: IL-33/ST2 signaling contributes to radicular pain by modulating MAPK and NF- κ B activation and inflammatory mediator expression in the spinal cord in rat models of noncompressive lumbar disk herniation. *J Neuroinflammation*, 2018; 15: 12
44. Kumamoto H, Ooya K: Expression of tumor necrosis factor alpha, TNF-related apoptosis-inducing ligand, and their associated molecules in ameloblastomas. *J Oral Pathol Med*, 2005; 34: 287–94
45. Ohta K, Naruse T, Ishida Y et al: TNF-alpha-induced IL-6 and MMP-9 expression in immortalized ameloblastoma cell line established by hTERT. *Oral Dis*, 2017; 23: 199–209